

Modeling of Textile Dye Removal from Wastewater Using Innovative Oxidation Technologies (Fe(II)/Chlorine and H₂O₂/Periodate Processes): Artificial Neural Network-Particle Swarm Optimization Hybrid Model

Abdelhalim Fetimi, Slimane Merouani, Mohd Shahnawaz Khan, Muhammad Nadeem Asghar, Krishna Kumar Yadav, Byong-Hun Jeon,* Mourad Hamachi, Ounissa Kebiche-Senhadji, and Yacine Benguerba*



Cite This: *ACS Omega* 2022, 7, 13818–13825



Read Online

ACCESS |



Metrics & More

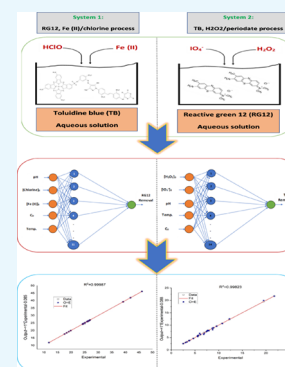


Article Recommendations



Supporting Information

ABSTRACT: An efficient optimization technique based on a metaheuristic and an artificial neural network (ANN) algorithm has been devised. Particle swarm optimization (PSO) and ANN were used to estimate the removal of two textile dyes from wastewater (reactive green 12, RG12, and toluidine blue, TB) using two unique oxidation processes: Fe(II)/chlorine and H₂O₂/periodate. A previous study has revealed that operating conditions substantially influence removal efficiency. Data points were gathered for the experimental studies that developed our ANN-PSO model. The PSO was used to determine the optimum ANN parameter values. Based on the two processes tested (Fe(II)/chlorine and H₂O₂/periodate), the proposed hybrid model (ANN-PSO) has been demonstrated to be the most successful in terms of establishing the optimal ANN parameters and brilliantly forecasting data for RG12 and TP elimination yield with the coefficient of determination (R²) topped 0.99 for three distinct ratio data sets.



1. INTRODUCTION

To remove organic pollutants, nutrients, and other impurities, a typical wastewater treatment plant uses a variety of physical, chemical, and biological unit processes. Detritus that is solubilized by microorganisms may only be removed using natural treatment.^{1,2} Industrial effluents are sometimes more challenging because of high organic matter content, non-neutral pHs, salinity, or the inclusion of synthetic chemicals with long persistence and low biodegradability.³ This treatment chain is suitable for the majority of household wastewaters. One of the most common occurrences is wastewater from the textile industry. The color is still discernible at low concentrations (less than 1 ppm for some dyes).^{4–7} Toxic, carcinogenic, mutagenic, or teratogenic compounds are often found in textile wastewater. For the most part, the chromophore grouping of a dye is employed to sort it out. Although anthraquinone, xanthene, phthalocyanine, and sulfur are also utilized, most chemicals are azo (–N=N–) derivatives.⁸ Some substances may alter wastewater treatment facilities, leading to more stable and harmful organisms, or they may not change and remain unchanged. For decades, scientists have been working to create advanced oxidation processes (AOPs) that are more environmentally friendly.^{9,10} Hydroxyl radical •OH, a potent oxidant ($E^\circ = 2,8$ V) and highly reactive species to most organic contaminants in situ, is produced by

AOPs. AOPs include the Fenton system (Fe(II)/H₂O₂), UV/H₂O₂, H₂O₂/O₃, UV/O₃, and UV/TiO₂.¹¹ An alternative to H₂O₂ and UV has recently been explored: the UV/chlorine procedure. It has been tried in a pilot or full-scale plant for water treatment, drinking water processing, and groundwater remediation.¹² In this process, several free radicals, including •OH, Cl₂•[–], and ClO•, are generated to collectively remove micropollutants at a much faster rate. Micropollutant elimination is an important goal for environmentalists and scientists alike. Utilizing multiple free radicals in a novel class of oxidation processes is one way to achieve this goal.¹³ As with UV/chlorine, UV/periodate acts as a multifree radical generator, producing radicals such as IO₃•, IO₄•, •OH, IO₃, O(³P), O₃, and H₂O₂ for the removal of a variety of water contaminants.^{14–17}

To integrate the results of experiments, mathematic models were regarded as appropriate. Kinetic modeling models have many constraints because of their complicated nature and

Received: January 5, 2022

Accepted: March 15, 2022

Published: April 15, 2022

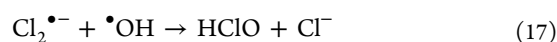
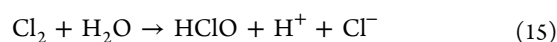
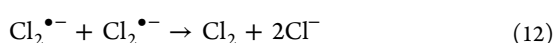
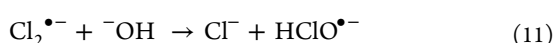
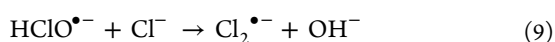
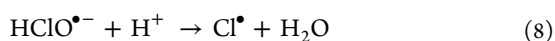
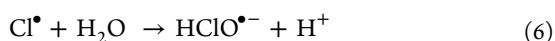
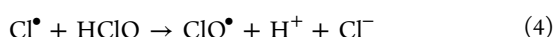
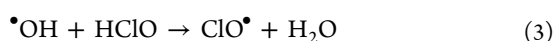
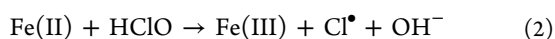
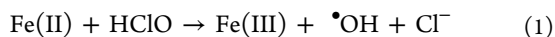


nonlinearity, limiting the parameters.^{18–27} Scientists have put out fuzzy logic (FL) models, artificial neural networks (ANNs), and other ML techniques. The latter have been applied to processes in several studies.^{28–36} Machine learning (ML) offers practical solutions to solve challenging issues in various industrial applications.⁴ ML includes computer algorithms and statistical methods required for data-driven control, estimation, prediction, classification, or clustering.³⁷

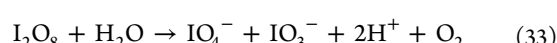
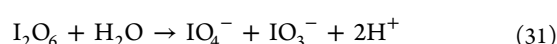
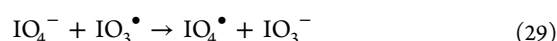
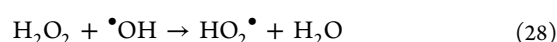
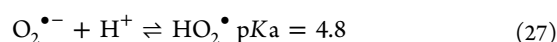
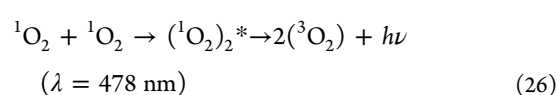
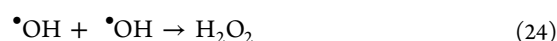
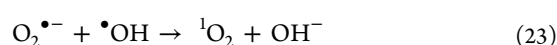
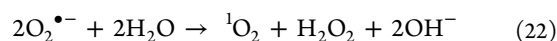
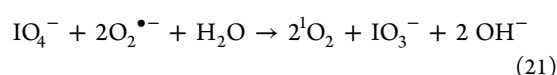
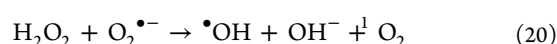
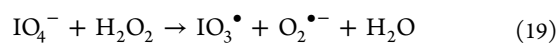
Although it is not practicable, complicated problems that were difficult to describe and analyze may now be appraised using these methods.³⁸ Several ANNs, such as a multilayer perceptron, are based on the human brain (MLP). This rigorous mathematical model often used in ML may explain any nonlinear relationship between input and output sets. An ANN is a collection of neurons linked by two fundamental parameters (connection weights and thresholds).^{39–41} Neural network techniques such as Levenberg–Marquardt (LM), scaled gradient descent (SGD), and gradient descent with momentum (GDWM) are among the most often employed (GDM). Adaptation, learning, and generalization may occur even when working with nonlinear functions. Contrarily, the speed of convergence of BPNN algorithms is slow. Some metaheuristic optimization approaches, such as the genetic algorithm (GA), firefly algorithm (FA), ant colony optimization (ACO), particle swarm optimization (PSO), and differential evolution (DE), may be utilized to solve these problems. They help the ANN find more optimal solutions faster, increasing its overall efficiency. Techniques like PSO and GA illustrate this trend.^{40,41} To cope with the most complex and complicated issues in optimization, they are the most promising global optimization approaches.^{42–46}

They have recently discovered two new oxidation methods for efficiently removing textile colors from wastewater.^{47,48} These two reactions, Fe(II)/chlorine and H₂O₂/periodate, have been discovered as multiple sources of free-radical oxidation of organic contamination. Cl[•], ClO[•], and Cl₂^{•-} chlorine radicals have been implicated in the Fe(II)/Chlorine process,^{38,39} while IO₃[•] and IO₄[•] iodine radicals, as well as singlet oxygen (¹O₂), have been implicated in the H₂O₂/periodate system.^{47,49}

• Fe(II)/chlorine process



• H₂O₂/periodate



To degrade RG12 and TB textile colors fast, we used Fe(II)/chlorine and H₂O₂/periodate processes. Several operational variables, including as reagent dosages, solution temperature, and pH, were examined throughout a wide range of reaction times. Industrial applications need a modeling technique that maximizes the efficiency of both kinetic processes.

This work aimed to develop a hybrid model (ANN-PSO) for the case of the removal of RG12 and TB dyes from wastewater utilizing Fe(II)/chlorine and H₂O₂/periodate oxidation processes. The PSO metaheuristic optimization was combined with ANN to construct a feasible model for predicting and optimizing the removal of textile colors from wastewater effluent using Fe(II)/chlorine and H₂O₂/periodate, respectively. The model's adaptability and durability were shown using the R² coefficient and the root mean square error (RMSE) between the predicted and experimental datasets.

2. EXPERIMENTAL DATA

Merouani et al.^{47,48} developed the ANN-PSO model by assessing the removal kinetics of RG12 and TB dyes from aqueous solutions under different experimental settings, utilizing the Fe(II)/chlorine and H₂O₂/periodate oxidation systems, respectively. The testing methodology and data are summarized in Text S1 in the Supporting Information.

For the Fe(II)/chlorine system, 146 datasets were collected from the experimental assessment of the removal kinetics of RG12 over time under various experimental factors such as solution pH (3–7.9), chlorine dosage (25–250 mM), Fe(II) initial concentration (5–100 M), initial RG12 concentration (C_0 : 10–100 mg/L), and liquid temperature (20–40 °C). For H₂O₂/periodate, 169 datasets were collected from the experimental assessment of TB removal kinetics over time under various experimental factors: initial H₂O₂ concentration (10–200 mM); initial periodate dosage (0.5–10 mM); initial solution pH (3–10.5); initial TB concentration (C_0 : 5–50 mg/L); and liquid temperature (10–50 °C).

3. MATERIALS AND METHODS

3.1. ANN Methodology. Input (IL), output (OL), and intermediate or hidden (HL) layers (Figures S1 and S2 of the

Table 1. Data Distribution of RG12 and TB Removal into Three Sets

divide rand	percentage (%)	divide data
<i>system 1: RG12, Fe(II)/chlorine process</i>		
train ratio	70	102
test ratio	15	22
validation ratio	15	22
<i>system 2: TP, H₂O₂/periodate process</i>		
train ratio	70	119
test ratio	15	25
validation ratio	15	25

Table 2. Range of All Parameters

parameters	minimum value	maximum value
<i>system 1: RG12, Fe(II)/chlorine process</i>		
IL		
pH	3	8
[chlorine] ₀ (μM)	25	1000
[Fe(II)] ₀ (μM)	0	100
C ₀ (mg/L)	10	100
temp. (°C)	10	40
OL		
RG12 removal (mg/L)	3.59	44.26
<i>system 2: TB, H₂O₂/periodate process</i>		
IL		
[H ₂ O ₂] ₀ (mM)	3	8
[IO ₄ ⁻] ₀ (mM)	25	1000
pH	3	11
temp. (°C)	10	50
C ₀ (mg/L)	5	50
OL		
TB removal (mg/L)	2.04	22

Supporting Information) are the three architectural levels of ANNs.^{51,53,54} Neurons (or nodes) are essential computer components used in parallel computing.^{53–55} Neurons work together to detect input data sets commonly seen.⁵⁶

$$y_i = f\left(\sum x_j \cdot w_{ij}\right) + \theta_j \quad (35)$$

f is the transfer function; x_j is the neuron's inputs; and w_{ij} is the link between IL and HL (weights) and the HL's threshold of j neuron.^{50,53} Constructing and training neuronal networks has as its primary goal the minimization of the objective function (or fitness function), which in turn leads to better predictions for new input.^{52,57} The latter compares the output and experimental data sets to determine how well the network operates. The fitness (error) function may thus be written as follows:

$$\text{RMSE} = \sqrt{\frac{\sum_{i=1}^n (y_i - y_o)^2}{N}} \quad (36)$$

N is the number of experiments, and y_i and y_o are the calculated and experimental data, respectively.⁵⁷

3.2. Particle Swarm Optimization. It is a nature-inspired evolutionary computing technology based on the movement and intelligence of swarms, such as ants and birds.³⁸ Kennedy and Eberhart created PSO in 1995 as a resilient stochastic optimization approach. Numerous optimization problems, such as function optimization, fuzzy control, and pattern recognition, have been solved using this approach.^{58,59}

Arbitrary particles, also known as solutions, are supported by the PSO algorithm. The search space (or the state space) is transformed into a swarm that seeks only the most advantageous options. The PSO training iteration uses the experience of individual particles and those around them to adjust their position and speed.

$$V_{id}^{n+1} = w \cdot V_{id}^n + c_1 \cdot \text{rand}_1 \cdot (Pbest_{id}^n - X_{id}^n) + c_2 \cdot \text{rand}_2 \cdot (Gbest_{id}^n - X_{id}^n) \quad (37)$$

$$X_{id}^{n+1} = X_{id}^n + V_{id}^{n+1} \quad (38)$$

V_{id}^{n+1} is the new velocity; $Pbest_{id}^n$ is the best position of the particle during training; $Gbest_{id}^n$ is the best position among all the particles in the swarm during the training iteration. The cognitive influence is $Pbest_{id}^n - X_{id}^n$ and the social influence is $Gbest_{id}^n - X_{id}^n$. c_1 and c_2 (acceleration constants) are the cognition and social weights, respectively.

w is the inertia weight (or inertia constant).⁶⁰ rand_1 and rand_2 generate random values ranging from 0 to 1. An example of the standard flow chart for the PSO approach may be seen in Figure S3 (Supporting Information).

The fundamental idea behind the PSO approach is that each particle is accelerated toward its $Pbest_{id}^n$ and $Gbest_{id}^n$ positions at each iteration.

When searching for the k -dimension and m -size of the acceleration, each particle may be represented as follows: $X_i = (x_{i1}, x_{i2}, \dots, x_{iD})^T$; $V_i = (v_{i1}, v_{i2}, \dots, v_{iD})$ (see Figure S4 in the Supporting Information).

3.3. PSO Approach. Analysis of state space is carried out by using a collection of particles. Weights and thresholds are stored in each particle for later adjustment.³⁹

Figure S5 of the Supporting Information shows the crucial phases of the ANN-PSO hybrid algorithm.

1. Importing experimental data.
2. Define ANN structure, weights, and thresholds.
3. Compute the number of weights and thresholds:

$$Z = A \cdot B + B \cdot C + B + C \quad (39)$$

Table 3. Optimal ANN-PSO Parameters (System 1: RG12, Fe(II)/Chlorine Process)

w_{ij}	1	2	3	4	5	6	7	8	9	10	11
1	-1.91	1.395	-0.742	0.878	-0.695	-1.91	1.547	-0.42	0.419	1.91	0.408
2	1.709	-0.568	-0.803	1.91	-1.691	-0.101	1.344	1.285	0.839	-1.896	-1.004
3	-0.318	-0.817	0.333	0.073	-1.054	-1.91	0.516	-1.91	-0.216	-1.08	0.879
4	1.67	1.69	-1.91	-1.157	1.91	-1.91	-1.91	0.291	1.91	-1.231	0.307
5	-1.239	0.936	-0.122	-1.503	0.994	1.91	-1.91	0.463	1.91	-0.42	-1.91
w_{1j}	1	2	3	4	5	6	7	8	9	10	11
1	1.049	-1.446	-0.993	1.615	0.436	-0.271	-0.357	-1.91	0.822	0.992	-1.727
θ_j	1	2	3	4	5	6	7	8	9	10	11
1	-1.097	-0.193	-1.447	1.8	-1.734	0.669	-0.585	-1.293	0.855	1.119	1.91
θ_1	-1.097										

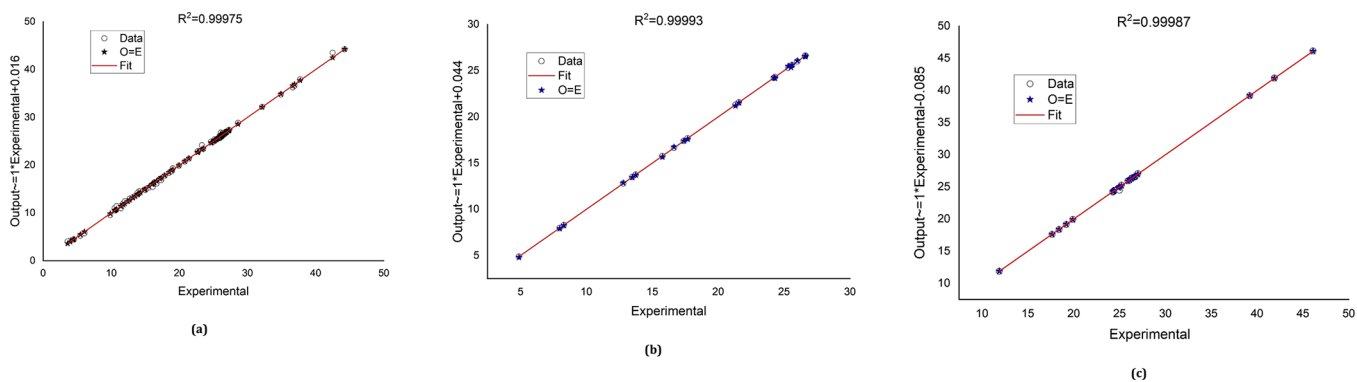
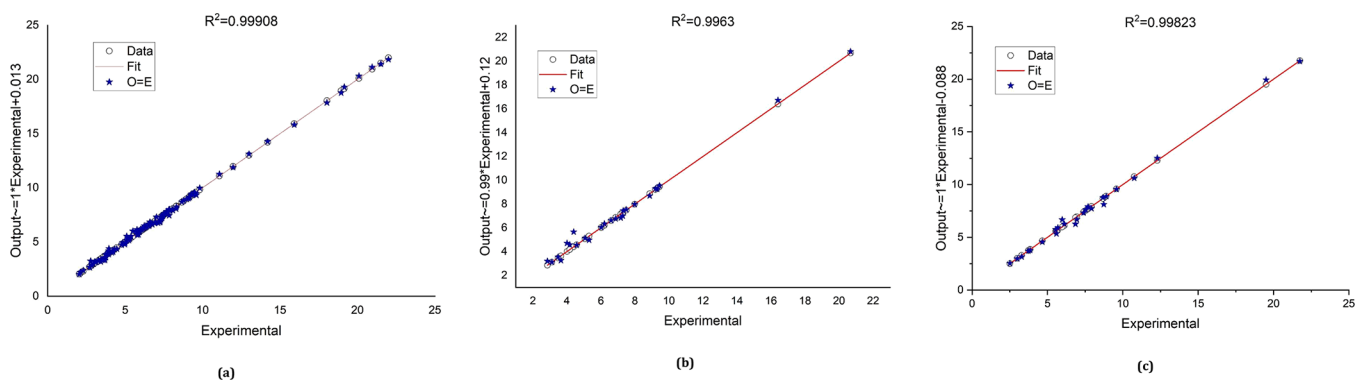


Figure 1. Regression plot of the output (ANN-PSO) and experimental data sets (System 1: RG12, Fe(II)/chlorine process): (a): training, (b): testing, and (c): validation.

Table 4. Optimal Weights and Thresholds of ANN Using the PSO Algorithm (System 2: TP, H₂O₂/Periodate Process)

w_{ij}	1	2	3	4	5	6	7	8	9	10	11	12	13	14
1	-0.770	0.900	-0.395	1.310	1.310	-1.163	0.771	1.310	-0.941	-0.317	-0.182	1.310	1.163	-1.310
2	0.193	1.310	-0.549	-1.310	0.699	0.956	0.546	0.763	-1.116	0.955	1.214	0.696	-0.217	0.288
3	-1.020	0.487	0.178	-1.310	0.706	-0.273	-0.597	0.259	-1.310	0.682	0.274	0.485	-1.310	-1.021
4	-0.432	1.031	-1.910	1.310	1.310	-0.035	0.544	0.603	-1.310	0.064	-0.422	-0.355	-1.310	0.310
5	0.252	1.310	-1.310	0.149	-1.310	0.751	-0.163	-0.435	-0.908	-0.358	0.235	-0.287	0.521	0.212
w_{1j}	1	2	3	4	5	6	7	8	9	10	11	12	13	14
1	-1.067	0.132	-1.190	0.115	-0.059	-0.886	-1.310	-1.310	-1.310	-0.057	0.938	0.846	0.216	1.310
θ_j	1	2	3	4	5	6	7	8	9	10	11	12	13	14
1	-1.094	0.965	-1.310	-1.197	-1.310	0.261	-1.261	0.391	1.310	1.310	1.300	0.256	-0.623	-0.612
θ_1	-1.094													

Figure 2. Regression plot of the output (ANN-PSO) and experimental data sets (System 2: TP, H₂O₂/periodate process): (a): training, (b): testing, and (c): validation.

3. A, B, and C are for IL, HL, and OL, respectively.
4. Initialize parameters.
5. Calculate the error, $Pbest$ and $Gbest$.

6. Adjust the location and velocity (eqs 37 and 38).
7. If $f(X_{id}^{n+1}) < f(Pbest_{id}^n)$ Then $Pbest_{id}^{n+1} = X_{id}^{n+1}$
Else $Pbest_{id}^{n+1} = Pbest_{id}^n$

8. If $f(X_{id}^{n+1}) < f(Gbest_{id}^n)$ Then $Gbest_{id}^{n+1} = X_{id}^{n+1}$
Else $Gbest_{id}^{n+1} = Gbest_{id}^n$
9. The ANN parameters' results are shown (weights, thresholds).

3.4. Database and Termination Criteria. Table 1 illustrates how the 146 experimental datasets for the Fe(II)/chlorine system and the 169 H₂O₂/periodate system were split into 70% training, 15% testing, and 15% validation. Initial solution pH, initial chlorine (or H₂O₂) concentration, initial Fe(II) (or periodate) concentration, initial RG12 (or TB) concentration, and initial liquid temperature are all factors in the IL. The removal efficiency of RG12 (or TP) is saved in the OL (see Table 2).

To evaluate or confirm the algorithm's halting conditions, the stopping criteria of this algorithm is considered or validated when the maximum number of iteration or minimum RMSE is attained.

4. RESULTS AND DISCUSSION

It is feasible to assess whether or not the mathematical model's predictions stand up under investigation using experimental

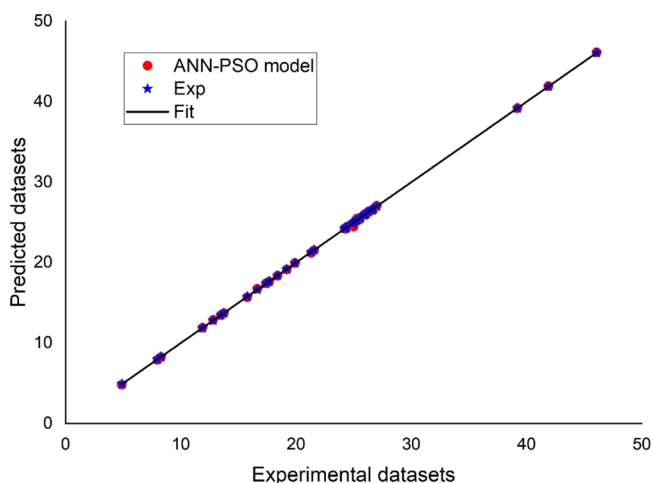


Figure 3. ANN-PSO-predicted datasets against experimental data sets (System 1: RG12, Fe(II)/chlorine process).

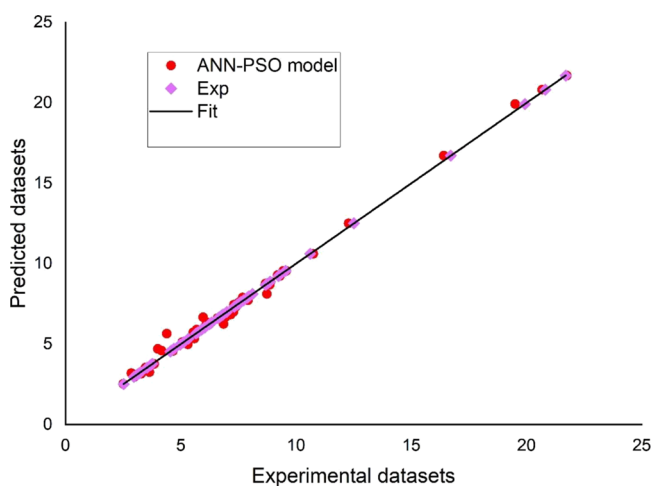


Figure 4. Plot of ANN-PSO predicted datasets against experimental data sets (System 2: TP, H₂O₂/periodate process).

data. Training the ANN-PSO hybrid model necessitates altering the number of neurons in the intermediate. Transfer functions are sigmoid in both the HL and OL. Most optimization strategies use it as a fitness function when assessing the proposed model's training performance. We are searching for parameters (weights and thresholds) that minimize the objective function (RMSE) between the anticipated outcomes of our models and the experimental datasets.

4.1. Fe(II)/Chlorine System. The five parameters in the IL were initial solution pH (from 3 to 7.9), initial chlorine concentration (from 25 to 1000 M), initial Fe(II) concentration (from 0 to 100 M), initial RG12 concentration (from 10 to 100 mg/L), and liquid temperature (from 10 to 40 °C). The OL includes RG12 removal (3.59–44.26 mg/L).

The best optimal parameters were c_1 and c_2 , of 1.25 and 2.5, respectively. $w = 0.15$; maximum number of iterations = 4500, and swarm size is 15:

- Fifty-five weights, w_{ij} (11×5) correlating IL with HL.
- Eleven weights, w_{j1} correlating HL with OL.
- Eleven thresholds, θ_j for HL's neurons.
- One threshold θ_1 for the OL (see Table 3).

Consequently, a 5:11:1 network (three layers) is the ultimate architectural network (i.e., five nodes in the IL, one HL with eleven nodes, and one node in the OL, respectively). After each training iteration, two variables, $Pbest$ and $Gbest$, determine how each solution changes its position and velocity. The RMSE objective function assesses the model's prediction ability by minimizing the difference between the actual and predicted data sets. As seen in Figure 1a, the ANN-PSO hybrid model presents and updates parameters (weights and thresholds) following its objective function, determining the output datasets throughout training. In Figure 1b, it can be seen how a network's performance is evaluated when training is completed using a network test. Data sets for RG12 removal from wastewater treatment concentrations are forecasted using network validation in Figure 1c.

Figure 1 demonstrates the network output from the proposed mathematical ANN-PSO model, and the experimental data sets for the three stages (training, testing, and validation) generated using MATLAB software. The practical data sets were classified into three types: training data sets (70%), testing data sets (15%), and validation data sets (15%). For the three phases, the coefficients of determination (R^2) are 0.99975, 0.99993, and 0.99987. The RMSE for each stage (training, testing, and validation) is 0.00181, 0.00084, and 0.00129, respectively. These statistics demonstrate strong performance across all data sets, with (R^2) values closer to unity and an RMSE less than 0.0012. This shows that all data fall along a 45-degree line with a slope = 1. The network outputs generated by the ANN-PSO hybrid model and relevant experimental data sets have the same linear connection (perfect correlation, "Perfect fit").

4.2. H₂O₂/Periodate System. The initial H₂O₂ concentration (10–200 mM), initial IO₄⁻ concentration (from 0.5 to 10 mM), initial solution pH (3–11), liquid temperature (10–50 °C), and initial TB concentration (5–50 mg/L) were the five parameters in the IL. The elimination quantity in the OL is 2.04–22 mg/L.

Table 4 shows the most optimum parameters of the ANN model derived using the PSO method (c_1 and c_2 equal to 1.25

Table 5. Comparison of ANN-PSO Results Obtained for Both Systems

models	ANN model design	R^2			RMSE		
		training	testing	validation	training	testing	validation
ANN-PSO: system 1 ^a	05/11/2001	0.99975	0.99993	0.99987	0.00181	0.00084	0.00129
ANN-PSO: system 2 ^b	5-14-1	0.99908	0.9963	0.99823	0.00174	0.0035	0.00273

^aRG12, Fe(II)/chlorine process. ^bTP, H₂O₂/periodate process.

and 2.5, respectively, $w = 0.25$, a maximum number of iterations = 4500, and swarm size = 15).

They are distributed as follows:

- w_{ij} (70 = 14 × 5) correlating IL with HL.
- w_{j1} (14) correlating HL with OL.
- θ_j (14) for HL's neurons.
- θ_1 (1) for OL.

The final architectural network is three layers: (5:14:1) network.

Figure 2 depicts the proposed mathematical ANN-PSO model's network output and the associated experimental data sets for the system H₂O₂/period throughout the three stages (training, testing, and validation) using MATLAB software. The practical data sets were classified into three types: training data sets (70%), testing data sets (15%), and validation data sets (15%).

The coefficient of determination, R^2 , was 0.99908, 0.9963, and 0.99823 for the three stages, respectively. The RMSE values for the three stages (training, testing, and validation) were 0.00174, 0.00350, and 0.00273, respectively. It is determined that the correlation is perfect because R^2 is near one and RMSE values are less than 0.0018.

Figures 3 and 4 compare the numerically simulated RG12 and TB removal (i.e., RG12 removal and TB Removal datasets) to the experimental data sets. The best fitting of the experimental data was also obtained for the two cases, revealing the ability of the ANN-PSO model toward predicting RG12 and TB removal.

For new RG12 data sets, Fe(II)/chlorine and H₂O₂/periodate processes were predicted more precisely using the ANN-PSO model. Table 5.

It can be concluded that the experimental and simulated findings agreed very well.

5. CONCLUSIONS

This work investigates the use of a new approach based on an ANN and PSO method to remove RG12 and TB dyes from wastewater utilizing Fe(II)/chlorine and H₂O₂/periodate oxidation processes. The ANN training function adjusts the weights and threshold values according to the PSO approach. The use of MATLAB software carried out the results. The coefficient of determination (R^2) from the ANN-PSO hybrid mathematical model topped 0.99 for three distinct ratio data sets from two independent systems. The proposed ANN-PSO model effectively predicts new RG12 and TB removal data sets with high (R^2) and low RMSE values.

■ ASSOCIATED CONTENT

Supporting Information

The Supporting Information is available free of charge at <https://pubs.acs.org/doi/10.1021/acsomega.2c00074>.

Experimental and data collection, different experimental runs for the removal of RG12 (mg/L) using the Fe(II)/chlorine oxidation system, different experimental runs

for the removal of TB (mg/L) using H₂O₂/periodate oxidation system, ANN topology, standard flow chart of the PSO algorithm, concept of changing a particle's position in PSO, and flow chart of the ANN-PSO hybrid mathematical model (PDF)

■ AUTHOR INFORMATION

Corresponding Authors

Byong-Hun Jeon – Department of Earth Resources and Environmental Engineering, Hanyang University, Seoul 04763, Republic of Korea; Email: bhjeon@hanyang.ac.kr

Yacine Benguerba – Department of Process Engineering, Faculty of Technology, University Ferhat ABBAS Setif-1, 19000 Setif, Algeria; orcid.org/0000-0002-8251-9724; Email: benguerbayacine@yahoo.fr

Authors

Abdelhalim Fetimi – Laboratoire des Procédés Membranaires et des Techniques de Séparation et de Récupération, Faculté de Technologie, Université de Bejaia, 06000 Bejaia, Algeria

Slimane Merouani – Laboratory of Environmental Process Engineering, Department of Chemical Engineering, Faculty of Process Engineering, University Constantine 3 – Salah Boubnider, 25000 Constantine, Algeria

Mohd Shahnawaz Khan – Department of Biochemistry, College of Science, King Saud University, Riyadh 11451, Saudi Arabia; orcid.org/0000-0002-4599-5924

Muhammad Nadeem Asghar – Department of Medical Biology, University of Québec at Trois-Rivieres, Trois-Rivieres, Québec G9A 5H7, Canada

Krishna Kumar Yadav – Faculty of Science and Technology, Madhyanchal Professional University, Bhopal 462044, India; orcid.org/0000-0002-4228-2726

Mourad Hamachi – Laboratoire des Procédés Membranaires et des Techniques de Séparation et de Récupération, Faculté de Technologie, Université de Bejaia, 06000 Bejaia, Algeria

Ounissa Kebiche-Senhadji – Laboratoire des Procédés Membranaires et des Techniques de Séparation et de Récupération, Faculté de Technologie, Université de Bejaia, 06000 Bejaia, Algeria

Complete contact information is available at: <https://pubs.acs.org/doi/10.1021/acsomega.2c00074>

Notes

The authors declare no competing financial interest.

■ ACKNOWLEDGMENTS

M.S.K. acknowledges the generous support from Research Supporting Project (RSP-2021/352) by King Saud University, Riyadh, Kingdom of Saudi Arabia.

REFERENCES

- (1) Henze, M.; van Loosdrecht, M.C.M.; Ekama, G. A.; Brdjanovic, D. *Biological wastewater treatment: principles, modelling and design*; IWA Publishing: United Kingdom, 2008; pp 1–511.
- (2) Sarayu, K.; Sandhya, S. Current Technologies for Biological Treatment of Textile Wastewater—A Review. *Appl. Biochem. Biotechnol.* **2012**, *167*, 645–661.
- (3) Ameta, S. C.; Ameta, R., Eds.; *Advanced oxidation processes for wastewater treatment: emerging green chemical technology*, 2nd ed.; Academic Press: United Kingdom, 2018; pp 1–412.
- (4) Guzman-Duque, F.; et al. Effects of sonochemical parameters and inorganic ions during the sonochemical degradation of crystal violet in water. *Ultrason. Sonochem.* **2011**, *18*, 440–446.
- (5) Li, Z.; Sellaoui, L.; Franco, D.; Netto, M. S.; Georjin, J.; Dotto, G. L.; Bajahzar, A.; Belmabrouk, H.; Bonilla-Petriciolet, A.; Li, Q. Adsorption of hazardous dyes on functionalized multiwalled carbon nanotubes in single and binary systems: Experimental study and physicochemical interpretation of the adsorption mechanism. *Chem. Eng. J.* **2020**, *389*, No. 124467.
- (6) Brião, G. V.; Jahn, S. L.; Foletto, E. L.; Dotto, G. L. Highly efficient and reusable mesoporous zeolite synthesized from a biopolymer for cationic dyes adsorption. *Colloids Surf., A* **2018**, *556*, 43–50.
- (7) Dotto, G. L.; Vieira, M. L.; Gonçalves, J. O.; Pinto, L. A. Remoção dos corantes azul brilhante, amarelo crepúsculo e amarelo tartrazina de soluções aquosas utilizando carvão ativado, terra ativada, terra diatomácea, quitina e quitosana: estudos de equilíbrio e termodinâmica. *Quim. Nova* **2011**, *34*, 1193–1199.
- (8) Carmen, Z.; Daniela, S. *Textile organic dyes-characteristics, polluting effects and separation/elimination procedures from industrial effluents—a critical overview*; IntechOpen: Croatia, 2012; pp 55–86.
- (9) Remucal, C. K.; Manley, D. Emerging investigators series: the efficacy of chlorine photolysis as an advanced oxidation process for drinking water treatment. *Environ. Sci.: Water Res. Technol.* **2016**, *2*, 565–579.
- (10) Glaze, W. H.; Kang, J. W. Advanced oxidation processes for treating groundwater contaminated with TCE and PCE: laboratory studies. *J. — Am. Water Works Assoc.* **1988**, *80*, 57–63.
- (11) Stefan, M. I., Ed.; *Advanced oxidation processes for water treatment: fundamentals and applications*; IWA publishing: United Kingdom, 2017; pp 1–681.
- (12) De Laat, J.; Stefan, M. *UV/Chlorine process*; IWA Publishing: London, 2018; pp 383–428.
- (13) Bendjama, H.; Merouani, S.; Hamdaoui, O.; Bouhelassa, M. Efficient degradation method of emerging organic pollutants in marine environment using UV/periodate process: case of chlorazol black. *Mar. Pollut. Bull.* **2018**, *126*, 557–564.
- (14) Weavers, L. K.; Hua, I.; Hoffmann, M. R. Degradation of triethanolamine and chemical oxygen demand reduction in wastewater by photoactivated periodate. *Water Environ. Res.* **1997**, *69*, 1112–1119.
- (15) Chia, L. H.; Tang, X.; Weavers, L. K. Kinetics and mechanism of photoactivated periodate reaction with 4-chlorophenol in acidic solution. *Environ. Sci. Technol.* **2004**, *38*, 6875–6880.
- (16) Tang, X.; Weavers, L. K. Decomposition of hydrolysates of chemical warfare agents using photoactivated periodate. *J. Photochem. Photobiol., A* **2007**, *187*, 311–318.
- (17) Tang, X.; Weavers, L. K. Using photoactivated periodate to decompose TOC from hydrolysates of chemical warfare agents. *J. Photochem. Photobiol., A* **2008**, *194*, 212–219.
- (18) Biswas, S.; Pathak, P. N.; Roy, S. B. Kinetic modeling of uranium permeation across a supported liquid membrane employing dinonyl phenyl phosphoric acid (DNPPA) as the carrier. *J. Ind. Eng. Chem.* **2013**, *19*, 547–553.
- (19) Kaya, A.; Alpoguz, H. K.; Yilmaz, A. Application of Cr (VI) transport through the polymer inclusion membrane with a new synthesized calix [4] arene derivative. *Ind. Eng. Chem. Res.* **2013**, *52*, 5428–5436.
- (20) Kaya, A.; Onac, C.; Alpoguz, H. K.; Yilmaz, A.; Atar, N. Removal of Cr (VI) through calixarene based polymer inclusion membrane from chrome plating bath water. *Chem. Eng. J.* **2017**, *283*, 141–149.
- (21) Kolev, S. D.; St John, A. M.; Cattrall, R. W. Mathematical modeling of the extraction of uranium (VI) into a polymer inclusion membrane composed of PVC and di-(2-ethylhexyl) phosphoric acid. *J. Membr. Sci.* **2013**, *425–426*, 169–175.
- (22) Kozłowski, C. A.; Walkowiak, W. Removal of chromium (VI) from aqueous solutions by polymer inclusion membranes. *Water Res.* **2002**, *36*, 4870–4876.
- (23) Meng, X.; Wang, C.; Zhou, P.; Xin, X.; Wang, L. Transport and selectivity of indium through polymer inclusion membrane in hydrochloric acid medium. *Front. Environ. Sci. Eng.* **2017**, *11*, 1–10.
- (24) Parhi, P. K. Supported liquid membrane principle and its practices: A short review. *J. Chem.* **2013**, *2013*, 1–11.
- (25) Yang, Q.; Kocherginsky, N. M. Copper removal from ammoniacal wastewater through a hollow fiber supported liquid membrane system: modeling and experimental verification. *J. Membr. Sci.* **2007**, *297*, 121–129.
- (26) Yang, X.; Duan, H.; Shi, D.; Yang, R.; Wang, S.; Guo, H. Facilitated transport of phenol through supported liquid membrane containing bis (2-ethylhexyl) sulfoxide (BESO) as the carrier. *Chem. Eng. Process.: Process Intensif.* **2015**, *93*, 79–86.
- (27) Kozłowski, C. A. Kinetics of chromium (VI) transport from mineral acids across cellulose triacetate (CTA) plasticized membranes immobilized by tri-n-octylamine. *Ind. Eng. Chem. Res.* **2007**, *46*, 5420–5428.
- (28) Le, L. T.; Nguyen, H.; Dou, J.; Zhou, J. A comparative study of PSO-ANN, GA-ANN, ICA-ANN, and ABC-ANN in estimating the heating load of buildings' energy efficiency for smart city planning. *Appl. Sci.* **2019**, *9*, 2630.
- (29) Moosavi, S. R.; Wood, D. A.; Ahmadi, M. A.; Choubineh, A. ANN-based prediction of laboratory-scale performance of CO₂-foam flooding for improving oil recovery. *Nat. Resour. Res.* **2019**, *28*, 1619–1637.
- (30) Gambhir, S.; Malik, S. K.; Kumar, Y. PSO-ANN based diagnostic model for the early detection of dengue disease. *New Horiz. Transl. Med.* **2017**, *4*, 1–8.
- (31) Ahmadi, M. A.; Bahadori, A.; Shadizadeh, S. R. A rigorous model to predict the amount of dissolved calcium carbonate concentration throughout oil field brines: side effect of pressure and temperature. *Fuel* **2015**, *139*, 154–159.
- (32) Geethanjali, M.; Slochanal, S. M.; Bhavani, R. PSO trained ANN-based differential protection scheme for power transformers. *Neurocomputing* **2008**, *71*, 904–918.
- (33) Ahmadi, M.; Chen, Z. Machine learning-based models for predicting permeability impairment due to scale deposition. *J. Pet. Explor. Prod. Technol.* **2020**, *10*, 2873–2884.
- (34) Ahmadi, M. A. Developing a robust surrogate model of chemical flooding based on the artificial neural network for enhanced oil recovery implications. *Math. Probl. Eng.* **2015**, *2015*, 1–9.
- (35) Ahmadi, M. A. Neural network based unified particle swarm optimization for prediction of asphaltene precipitation. *Fluid Phase Equilib.* **2012**, *314*, 46–51.
- (36) Ahmadi, M. A.; Soleimani, R.; Lee, M.; Kashiwao, T.; Bahadori, A. Determination of oil well production performance using artificial neural network (ANN) linked to the particle swarm optimization (PSO) tool. *Petroleum* **2015**, *1*, 118–132.
- (37) Khayyam, H.; Jamali, A.; Bab-Hadiashar, A.; Esch, T.; Ramakrishna, S.; Jalili, M.; Naebe, M. A novel hybrid machine learning algorithm for limited and big data modeling with application in industry 4.0. *IEEE Access* **2020**, *8*, 111381–111393.
- (38) Soleimani, R.; Shoushtari, N. A.; Mirza, B.; Salahi, A. Experimental investigation, modeling and optimization of membrane separation using artificial neural network and multi-objective optimization using genetic algorithm. *Chem. Eng. Res. Des.* **2013**, *91*, 883–903.

- (39) Bisi, M.; Goyal, N. K. *Artificial Neural Network Applications for Software Reliability Prediction*; John Wiley & Sons, 2017; pp 1–312.
- (40) Kim, P. *MATLAB Deep Learning: With Machine Learning, Neural Networks and Artificial Intelligence*, 1st ed.; Springer Science + Business Media: New York, 2017; pp 1–21.
- (41) Rakitianskaia, A. S. *Using particle swarm optimisation to train feedforward neural networks in dynamic environments*; Diss. University of Pretoria, 2012; pp 1–271.
- (42) Momeni, E.; Armaghani, D. J.; Hajihassani, M.; Amin, M. F. Prediction of uniaxial compressive strength of rock samples using hybrid particle swarm optimization-based artificial neural networks. *Measurement* **2015**, *60*, 50–63.
- (43) Ding, S.; Xu, L.; Su, C.; Jin, F. An optimizing method of RBF neural network based on genetic algorithm. *Neural Comput. Appl.* **2012**, *21*, 333–336.
- (44) Cheng, R.; Jin, Y. A social learning particle swarm optimization algorithm for scalable optimization. *Inf. Sci.* **2015**, *291*, 43–60.
- (45) Clerc, M.; Kennedy, J. The particle swarm-explosion, stability, and convergence in a multidimensional complex space. *IEEE Trans. Evol. Comput.* **2002**, *6*, 58–73.
- (46) El Sadek, H.; Zhang, X.; Rashad, M.; Cheng, C. Improvement of Interior Ballistic Performance Utilizing Particle Swarm Optimization. *Math. Probl. Eng.* **2014**, *2014*, 1–10.
- (47) Chadi, N. E.; Merouani, S.; Hamdaoui, O.; Bouhelassa, M.; Ashokkumar, M. H₂O₂/Periodate (IO₄⁻): A novel advanced oxidation technology for the degradation of refractory organic pollutants. *Environ. Sci.: Water Res. Technol.* **2019**, *5*, 1113–1123.
- (48) Meghlaoui, F. Z.; Merouani, S.; Hamdaoui, O.; Bouhelassa, M.; Ashokkumar, M. Rapid catalytic degradation of refractory textile dyes in Fe (II)/chlorine system at near neutral pH: radical mechanism involving chlorine radical anion (Cl₂⁻)-mediated transformation pathways and impact of environmental matrices. *Sep. Purif. Technol.* **2019**, *227*, No. 115685.
- (49) Meghlaoui, F. Z.; Merouani, S.; Hamdaoui, O.; Alghyamah, A.; Bouhelassa, M.; Ashokkumar, M. Fe (III)-catalyzed degradation of persistent textile dyes by chlorine at slightly acidic conditions: the crucial role of Cl₂⁻ radical in the degradation process and impacts of mineral and organic competitors. *Asia-Pac. J. Chem. Eng.* **2021**, *16*, No. e2553.
- (50) Chadi, N. E.; Merouani, S.; Hamdaoui, O.; Bouhelassa, M.; Ashokkumar, M. Influence of mineral water constituents, organic matter and water matrices on the performance of the H₂O₂/IO₄⁻-advanced oxidation process. *Environ. Sci.: Water Res. Technol.* **2019**, *5*, 1985–1992.
- (51) Gevrey, M.; Dimopoulos, I.; Lek, S. Review and comparison of methods to study the contribution of variables in artificial neural network models. *Ecol. Modell.* **2003**, *160*, 249–264.
- (52) Ranković, V.; Radulović, J.; Radojević, L.; Ostojčić, A.; Čomić, L. Neural network modeling of dissolved oxygen in the Gruža reservoir, Serbia. *Ecol. Modell.* **2010**, *221*, 1239–1244.
- (53) Fetimi, A.; Dêas, A.; Benguerba, Y.; Merouani, S.; Hamachi, M.; Kebiche-Senhadji, O.; Hamdaoui, O. Optimization and prediction of safranin-O cationic dye removal from aqueous solution by emulsion liquid membrane (ELM) using artificial neural network-particle swarm optimization (ANN-PSO) hybrid model and response surface methodology (RSM). *J. Environ. Chem. Eng.* **2021**, *9*, No. 105837.
- (54) Kiranyaz, S.; Ince, T.; Gabbouj, M. *Multidimensional particle swarm optimization for machine learning and pattern recognition*; Springer: Berlin, 2014; pp 1–321.
- (55) Jiang, J.; Trundle, P.; Ren, J. Medical image analysis with artificial neural networks. *Comput. Med. Imaging Graphics* **2010**, *34*, 617–631.
- (56) Eslamimanes, A.; Gharagheizi, F.; Mohammadi, A. H.; Richon, D. Artificial neural network modeling of solubility of supercritical carbon dioxide in 24 commonly used ionic liquids. *Chem. Eng. Sci.* **2011**, *66*, 3039–3044.
- (57) Alba, E., Martí, R., Eds.; *Metaheuristic procedures for training neural networks*; Springer Science & Business Media: New York, 2006; Vol. 36, pp 1–249.
- (58) Bonyadi, M. R.; Michalewicz, Z. Particle swarm optimization for single objective continuous space problems: a review. *Evol. Comput.* **2017**, *25*, 1–54.
- (59) Eberhart, R. C.; Shi, Y.; Kennedy, J. *Swarm intelligence*; Academic Press: United States of America, 2001; pp 1–497.
- (60) Gudise, V. G.; Venayagamoorthy, G. K. Comparison of particle swarm optimization and backpropagation as training algorithms for neural networks. In *Proceedings of the 2003 IEEE Swarm Intelligence Symposium, 03EX706*; IEEE, 2003; pp 110–117, 10.1109/SIS.2003.1202255.

Recommended by ACS

Continuous Heterogeneous Fenton-Type Process for Dye Pollution Abatement Intensified by Hydrodynamic Cavitation

Gabriel Salierno, María Alejandra Ayude, et al.

NOVEMBER 08, 2021
INDUSTRIAL & ENGINEERING CHEMISTRY RESEARCH

READ 

Effective Removal of Acid Dye in Synthetic and Silk Dyeing Effluent: Isotherm and Kinetic Studies

Elizaveta Sterenzon, Hadas Mamane, et al.

DECEMBER 30, 2021
ACS OMEGA

READ 

Hybrid System of Flocculation–Photocatalysis for the Decolorization of Crystal Violet, Reactive Red X-3B, and Acid Orange II Dye

Yuanfang Wang, Chen Liu, et al.

NOVEMBER 30, 2020
ACS OMEGA

READ 

Synergistic Mechanism of Combined Inhibitors on the Selective Flotation of Arsenopyrite and Pyrite

Xiaohao Sun, Hongyang Xu, et al.

FEBRUARY 10, 2022
ACS OMEGA

READ 

Get More Suggestions >